Journal of Chemical Crystallography
https://doi.org/10.1007/s10870-018-0732-4

ORIGINAL PAPER

Synthesis, Characterization, and Crystal Structure of (2*E*)-3-(4-Fluorophenyl)-1-(2-hydroxyphenyl)prop-2-en-1-one

Cathryn A. Slabber[1] · Craig D. Grimmer[2] · Orde Q. Munro[1] · Ross S. Robinson[2]

Received: 23 February 2015 / Accepted: 7 September 2018

Abstract

The title chalcone, of formula $C_{15}H_{11}F_1O_2$, crystallized in the orthorhombic space group $P2_12_12_1$ (# 19) with crystal parameters $a = 6.9998(8)$ Å, $b = 12.6740(15)$ Å, $c = 12.8997(15)$ Å, $V = 1144.4(2)$ Å^3, $Z = 4$, determined at 100 K with MoKα radiation. The solid-state structure displays an intramolecular S(6) hydrogen bond and the crystal architecture is maintained by intermolecular F···H, O···H, and C···C short contacts. A DFT geometry optimization is compared with the experimental structure. As ^{19}F NMR spectroscopy can be used for metabolic tagging of biologically active compounds (including chalcones), the solution-state ^{19}F chemical shift and $^{13}C^{19}F$ coupling constants (^nJ) are also reported.

Graphical Abstract

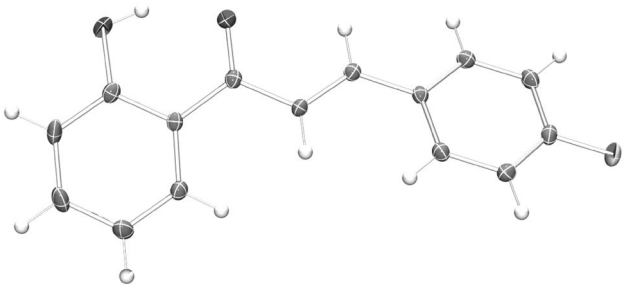

Keywords Chalcone · Hydrogen-bonding · DFT

Introduction

Chalcones are a class of natural products and synthetic compounds with a wide range of biological activities [1]. They are readily prepared by the base-catalysed Aldol [2] condensation of aldehydes and ketones with usually spontaneous dehydration of the ß-hydroxy ketone intermediate to form a conjugated enone. The title fluorinated chalcone [3, 4] has been prepared as an intermediate in the preparation of a novel range of cyclooxygenase (COX) inhibitors [5]. Fluorine atoms are found in 20–30% of modern drugs [6] and the inclusion of a fluorine atom in a pharmaceutical candidate not only allows the modification of electrostatic properties [7] but is also a means of metabolic tagging for study *via* ^{19}F NMR spectroscopy. Fluorine atoms can also impart a number of pharmaceutically appealing attributes to a drug [8]. Herein we report the synthesis and characterization of (2*E*)-3-(4-fluorophenyl)-1-(2-hydroxyphenyl)prop-2-en-1-one by multiple spectroscopic methods and a combination of single crystal X-ray diffraction and DFT simulations for

Electronic supplementary material The online version of this article (https://doi.org/10.1007/s10870-018-0732-4) contains supplementary material, which is available to authorized users.

✉ Ross S. Robinson
robinsonr@ukzn.ac.za

[1] School of Chemistry, University of the Witwatersrand, Johannesburg, South Africa

[2] School of Chemistry and Physics, University of KwaZulu-Natal, Pietermaritzburg, South Africa

Published online: 12 September 2018

structure elucidation and delineation of the electronic and magnetic properties of the compound.

Experimental

Measurements (NMR Spectroscopy)

NMR data were recorded on either a Bruker Avance-III 500 or Bruker Avance-III 400 spectrometer with ^{1}H freqencies of 500 MHz or 400 MHz, respectively, using a 5 mm ^{31}P^{109}Ag/{^{1}H} BBOZ probe. Data acquisition and processing were carried out with Bruker TopSpin software (v 2.1, pl 6). All proton and carbon chemical shifts are quoted in parts-per-million (ppm) and are measured relative to the position of the relevant solvent signal (DMSO-d_6, ^{1}H 2.50 ppm, ^{13}C 39.50 ppm) [9]. Coupling constants are reported in Hertz (Hz). All experiments were performed at 30 °C.

Measurements (X-ray Diffraction)

A suitable single crystal was suspended in Paratone [10] oil in a Mitegen [11] loop. X-ray diffraction data were collected with a Bruker Apex Duo diffractometer with an Incoatec IμS source [12] using Mo-Kα radiation at a temperature of 100 K. The structure was solved with Olex2 [13] by "Direct Methods" using ShelXS-1997 [14] and refined with ShelXL-1997 [14] using CGLS minimisation. Absorption correction was performed with SADABS [15]. Molecular measurements were determined with Olex2 [13], Mercury [16, 17], MacroModel [18, 19] and molecular visuals were created with Olex2 [13], PyMol [20] and POVRay [21]. The title chalcone is asymmetric, lacking any symmetry elements, permitting its crystallization in space group P212121. The nonplanar conformation of the asymmetric unit coupled with its absence of point chirality leads to its crystallization in a chiral space group. The absolute structure is not particularly relevant in the present case. However, the Flack parameter [22] was refined, as is customary in ShelXL for all chiral space groups, to give the correct absolute structure (enantiomer) within the standard uncertainty of the estimate.

Synthesis and Characterisation

Potassium hydroxide (0.662 g; 11.2 mmol) was added to ethanol (95%; 20 ml) and stirred until dissolved. To the solution was added slowly 2′-hydroxyacetophenone (0.549 g; 4.00 mmol), followed by 4-fluorobenzaldehyde (0.500 g; 4.00 mmol). The solution was stirred overnight at room temperature. Hydrochloric acid (2.0 M) was added to neutralize the solution and the yellow precipitate was isolated by suction filtration and allowed to air-dry overnight (Scheme 1) with a yield of 80% (melting point 116.5–118.5 °C; uncorrected). Translucent yellow crystals suitable for X-ray diffraction were obtained by slow evaporation of an ethanol solution. A SciFinder [23] search reveals 61 reports of the synthesis of this compound between 2001 [24] and 2018 [25] and yet the crystal structure is not present in the Cambridge Structural Database (May 2018).

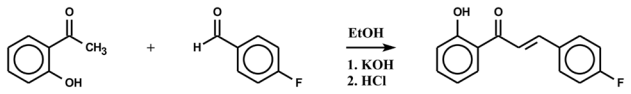

Scheme 1 Basic synthesis of title chalcone

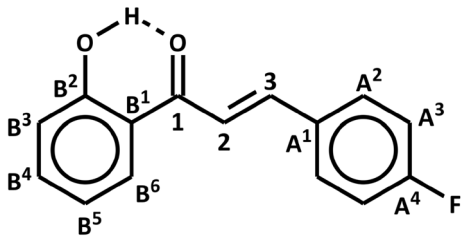

Fig. 1 Intramolecular S(6) hydrogen bond; chalcone ring nomenclature (A and B rings)

^{1}H NMR, DMSO-d_6 (assignments labelled as in Fig. 1): δ 6.99–7.01 (m, 1 H, B^3); 6.99–7.03 (m, 1 H, B^5), 7.29–7.34 (m, 2 H, A^3); 7.55–7.59 (m, 1 H, B^4); 7.84 (d, $^{3}J_{HH}$ = 15.6, 1 H, 3); 7.98–8.01 (m, 3 H, A^2 and 2); 8.25 (dd, J = 8.5 Hz, J = 1.6 Hz, 1 H, B^6); 12.48 (br.s, 1 H, OH).

^{13}C NMR, DMSOd_6 (assignments labelled as in Fig. 1): δ 115.95 (d, $^{2}J_{CF}$ = 21.8 Hz, A^3); 117.68 (s, B^3); 119.10 (s, B^5); 120.66 (s, B^1); 121.62 (d, $^{6}J_{CF}$ = 2.3 Hz, 2); 130.83 (s, B^6); 131.10 (d, $^{4}J_{CF}$ = 3.1 Hz, A^1); 131.51 (d, $^{3}J_{CF}$ = 8.7 Hz, A^2); 136.29 (s, B^4); 143.52 (d, $^{5}J_{CF}$ = 0.8 Hz, 3); 161.82 (s, B^2); 163.57 (d, $^{1}J_{CF}$ = 249.7 Hz, A^4); 193.52 (s, 1).

^{19}F-{^{1}H} NMR (DMSOd_6): δ 109.0 (s, 1 F, F).

HRMS: Calculated $C_{15}H_{11}O_2F_1$ 242.0743; found 241.0667 (M-1).

Results and Discussion

The summary of the single crystal diffraction data is presented in Table 1.

The molecular structure features a single intramolecular hydrogen bond O_2–H_2···O1, generating an S(6) ring motif [26, 27] (Fig. 1) with an angle between the plane of the S(6) ring and that of the B ring [28] of the chalcone of 1.4 (3)°.

The intramolecular hydrogen bond is maintained in solution, given the chemical shift of the phenolic proton at 12.48 ppm.

Table 1 Summary of crystal data

Formula	$C_{15}H_{11}F_1O_2$
Formula mass (g/mol)	242.24 (242.0743)
Crystal system	Orthorhombic
Space group	$P2_12_12_1$ (# 19)
a (Å)	6.9998 (8)
b (Å)	12.6740 (15)
c (Å)	12.8997 (15)
α, β, γ (°)	90
V (Å^3)	1144.4 (2)
Z	4
Temperature (K)	100 (2)
Radiation	Mo Kα
Wavelength	0.71073
Collected reflections	6675
2Θ range (°)	4.506, 56.504
Unique reflections	2790
R_{int}	0.0155
R_{sigma}	0.0196
R_1 (I > 2σ(I))	0.0296 (3%)
wR_2	0.0824
Flack parameter	0.0(2)
Crystal size (mm)	0.2 × 0.2 × 0.2
Crystal description	Clear, yellow shard

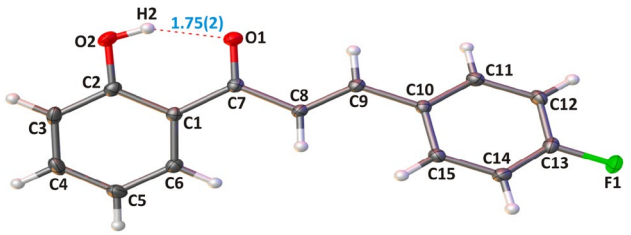

Fig. 2 Crystallographic atom labels; intramolecular S(6) H-bond; relative positions of the fluoro- and hydroxyl-substituents; configuration of alkene bond. Thermal ellipsoids at 50%

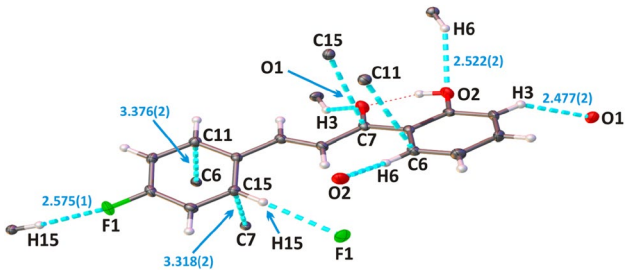

Fig. 3 The five short contacts of the intermolecular structure

The angle between the planes of the hydroxyl-substituted B ring and fluoro-substituted A ring of the chalcone is 29.88 (4)° and the torsion angles between the propene bridge and the A and B rings are 175.35 (10)° (C2C1C7C8), 169.03 (11)° (C1C7C8C9), and 164.92 (12)° (C8C9C10C11) culminating in a twisted, non-planar structure. The fluoro- and hydroxyl- substituents are placed on opposite sides of the molecule and the double bond of the propene fragment (C8C9) has an *E*- or *trans*-configuration (Fig. 2).

The *E*/*trans* configuration of the propene fragment is confirmed by the $^3J_{HH}$ coupling constant of 15.6 Hz [29] in the solution-state NMR spectrum.

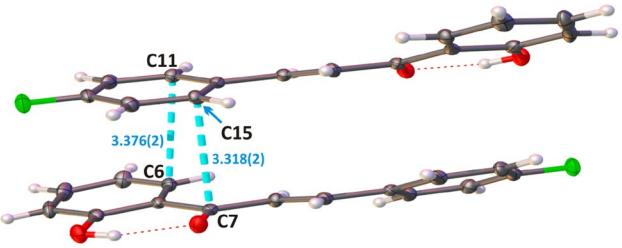

Fig. 4 Head-to-tail stacking of columns, viewed along the *b*-axis

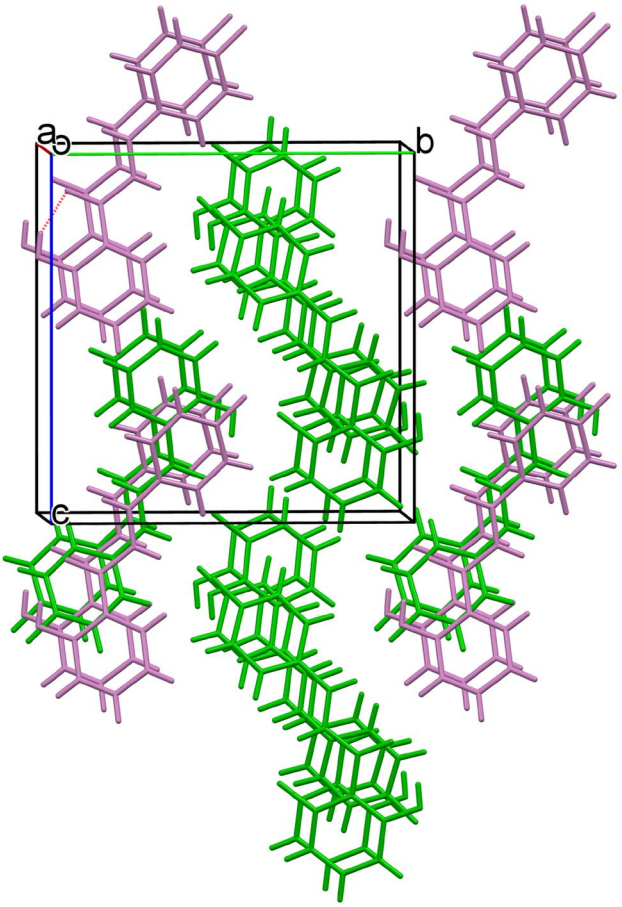

Fig. 5 Staggered arrangement of columns, coloured by symmetry operation, viewed along the *a*-axis

The bulk structure is characterized by five short contacts (Fig. 3): an F···H contact of 2.575 (1) Å, between the fluorine atom and H15 of the A ring, an O···H contact of 2.477 (2) Å between the oxygen atom of the carbonyl moiety (O1) and H3 of the B ring, an O···H contact of 2.522 (2) Å between the oxygen atom of the hydroxyl moiety (O2) and H6 of the B ring, a C···C contact of 3.318 (2) Å between the carbon atom of the carbonyl group (C7) and C15 of the A ring, and a C···C contact of 3.376 (2) Å between C11 of the A ring and C6 of the B ring.

Molecules are stacked in columns along the *a* axis (visible by viewing along the *b* axis; Fig. 4) in a slightly offset head-to-tail arrangement, with the two C···C short contacts between the A and B rings and the carbonyl group maintaining the columns. The planes of the A and B rings in each layer are not quite coplanar, with a between-plane angle of 4.16 (4)°, and a between-centroid spacing of 3.7837 (8) Å.

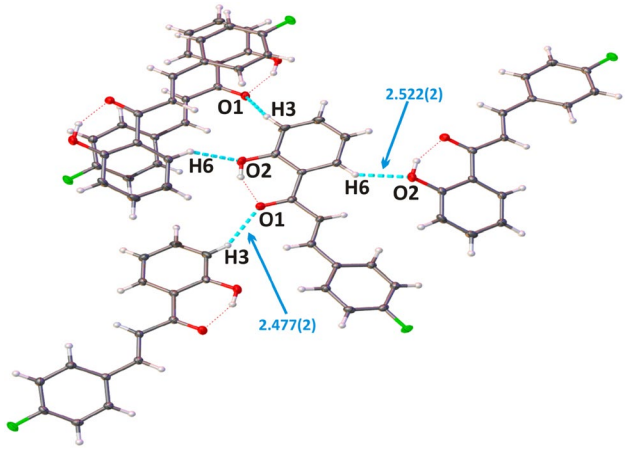

Fig. 6 Hydrogen bonding network of head-to-head O···H short contacts

Table 2 Crystal packing short contacts

Contact	Distance (Å)	Operations
C7–C15	3.318 (2)	±1/2 + x, 3/2 − y, 1 − z
C6–C11	3.376 (2)	±1/2 + x, 3/2 − y, 1 − z
H6–O2	2.522 (2)	± x, − 1/2 + y, 3/2 − z
F1–H15	2.575 (1)	1/2 − x, 1 − y, ± 1/2 + z
O1–H3	2.477 (2)	1/2 − x, 2 − y, ± 1/2 + z

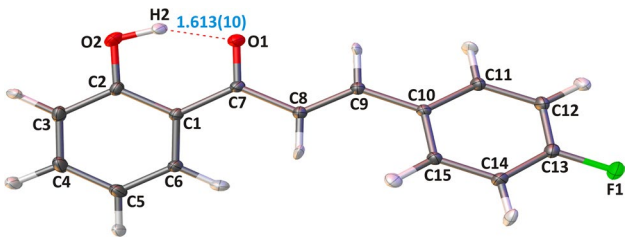

Fig. 7 Anisotropic H-atom placement by HAR (*cf* Fig. 2)

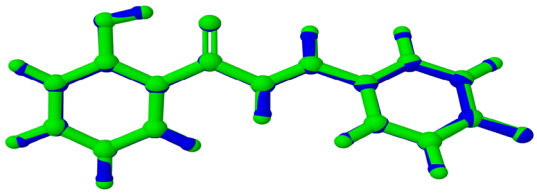

Fig. 8 Superposition (all atoms) of CSD (blue) and HAR (green) structures. RMSD 0.0864; maximum difference at atom H4

Table 3 H–X and H···X bond lengths

Bond (Å)	No HAR	HAR
O2–H2	0.852 (19)	0.987 (10)
O1···H2	1.75 (2)	1.613 (10)
C3–H3	0.95007 (8)	1.088 (7)
C4–H4	0.95004 (11)	1.118 (8)
C5–H5	0.95002 (9)	1.088 (7)
C6–H6	0.95005 (8)	1.056 (7)
C8–H8	0.94990 (10)	1.075 (8)
C9–H9	0.95003 (10)	1.094 (7)
C11–H11	0.95006 (10)	1.087 (7)
C12–H12	0.94998 (10)	1.072 (9)
C14–H14	0.95008 (10)	1.081 (8)
C15–H15	0.95008 (10)	1.068 (8)

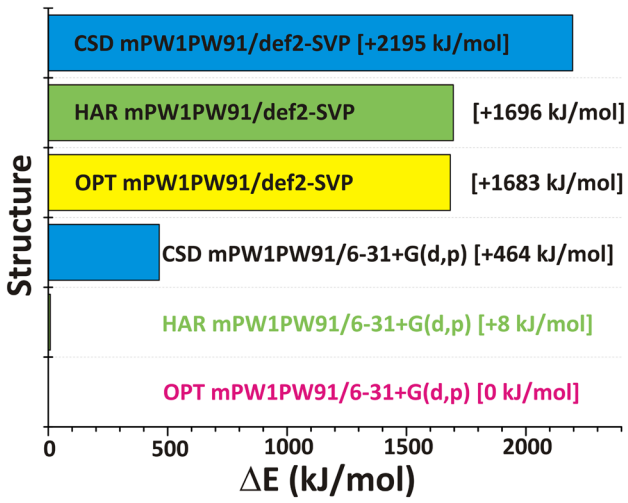

Fig. 9 Relative energies (ΔE, kJ/mol) of title molecule crystallographic structure with (HAR) and without (CSD) Hirschfeld Atom Refinement; DFT optimized structures

The columns are arranged in a staggered pattern, in two dimensions, visible along the *a* axis (Fig. 5), and are held together by the remaining three short contacts, tail-to-tail H···F, and two head-to-head O···H (Fig. 6).

Table 2 summarises the five short contacts with their respective distances and symmetry operations.

Hirschfeld Refinement and DFT Simulation

Hirschfeld Atom Refinement (HAR) with Olex2 [13] using the "Restricted Hartree–Fock" method with the def2-SVP basis set [30–32] yields an improved *R*-factor of 1.5% and anisotropic positioning of the hydrogen atoms (Fig. 7) with longer bond lengths for C–H and O–H connections and a single shorter O···H connection for the intramolecular hydrogen bond. (Fig. 8; Table 3).

Density functional theory (DFT) simulations of the molecular geometry were performed for comparison with the crystal structure, with and without HAR. The simulations were carried out using the mPW1PW91 [33] functional and the def2-SVP [30–32] basis set (used by the HAR in Olex2) and the 6–31 + G(d,p) basis set using the Gaussian-09 [34, 35] suite of programs. The in vacuo geometry optimisation was followed by a frequency calculation, the absence of negative frequencies indicating that the optimised geometry was at least a local minimum on the potential energy surface. The relative energies [36] of the CSD, HAR, and DFT optimized structures (OPT) are shown in Fig. 9, for the basis sets def2-SVP and 6–31 + G(d,p). For each basis set, the order of relative energies is the same, OPT < HAR < CSD.

Figure 10 illustrates the superposition using MacroModel [18, 19] of the experimental and theoretical structures and Table 4 shows the root-mean-square-deviation (RMSD) between the structures, compared on an "all atoms" basis, and the atom of maximum deviation.

Table 5 contains relevant parameters for the structures and Fig. 9 shows the relative energies.

The RMSD values (Table 4) indicate a relatively good match between the structures although the structures produced by the *in vacuo* DFT simulations are more planar and of lower energy, the greatest difference observed in the inter-plane angle between the A and B rings (30° vs 2°–4°; Table 5). Figure 11 illustrates this difference by superposition of the B-rings of the HAR and mPW1PW91/def2-SVP structures. The non-planarity arises from rotation of two bonds, C7–C8 and C9–C10, in the crystal structure.

The difference is attributed to the absence of the five intermolecular interactions (Fig. 3) from the single-molecule gas-phase simulation, particularly the hydrogen bonds (Fig. 6) and the C–H···F interactions (Fig. 3) responsible for the inter-column connections. In supermolecular architecture, hydrogen bonding is the prevalent interaction and, while there is debate on whether the C–H···F interaction can be termed a "hydrogen bond", "weak hydrogen bond", or a Van der Waal's interaction, this type of H···F interaction is significant in the structure of crystals [37–39] It is noteworthy that while H4 and H12 (Table 4) do not feature in the short contact interactions, H15 (Table 4) is a key feature of the inter-column architecture of the crystal, in the C–H···F interaction of 2.575 (1) Å [40].

The intramolecular H-bond (O2–H2···O1; Figs. 2, 7) is reproduced by the DFT simulation (Fig. 12).

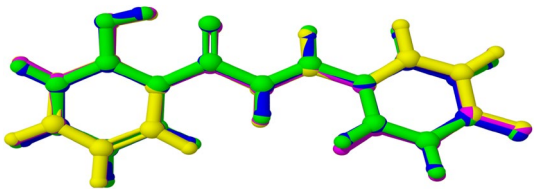

Fig. 10 Superposition (all atoms) of CSD (blue), HAR (green), OPT mPW1PW91/def2-SVP (yellow), OPT mPW1PW91/6–31 + G(d,p) (magenta) structures

Table 4 RMSD values for structure comparisons (atom of maximum difference)

	CSD	HAR	def2-SVP
CSD	–	0.0864 (H4)	0.3789 (H12)
HAR	0.0864 (H4)	–	0.3769 (H15)
def2-SVP	0.3789 (H12)	0.3769 (H15)	–
6–31 + G(d,p)	0.3538 (H12)	0.3515 (H15)	0.0266 (H15)

Table 5 Selected structural parameters

Parameter (°)	CSD	HAR	def2-SVP	6–31 + G(d,p)
Interplane angle, S(6) and B-ring	1.4	1.6	0.19	0.3
Interplane angle, A and B rings	29.9	29.9	2.2	4.0
Torsion, C2–C1–C7–C8	175.4	175.3	179.9	179.3
Torsion C1–C7–C8–C9	169.0	169.0	179.0	178.4
Torsion, C8–C9–C10–C11	164.9	165.0	179.0	178.1

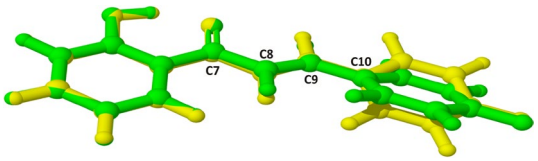

Fig. 11 Superposition of B-rings of HAR (green), OPT mPW1PW91/def2-SVP (yellow) structures

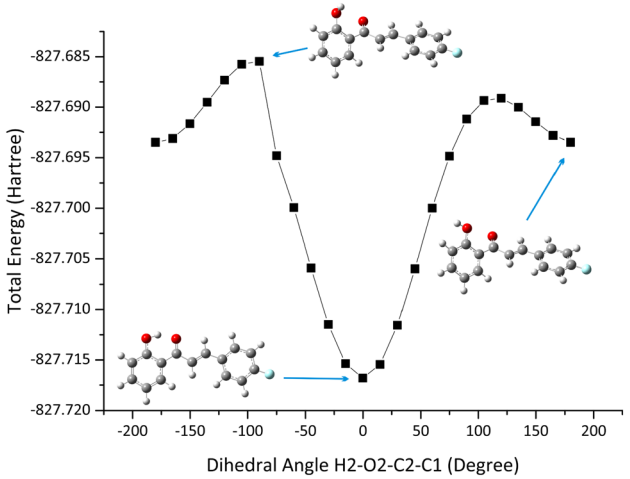

Fig. 12 Energy profile (mPW1PW91/def2SVP) of the intramolecular hydrogen bond, O2–H2···O1

Acknowledgements The authors acknowledge the support of the University of KwaZulu-Natal (Pietermaritzburg) and the National Research Foundation (NRF) of South Africa.

Compliance with Ethical Standards

Conflict of interest The authors declare that they have no conflict of interest.

References

1. Batovska DI, Todorova IT (2010) Trends in utilization of the pharmacological potential of chalcones. Curr Clin Pharmacol 5(1):1–29
2. Wurtz A (1872) Ueber einen Aldehyd-Alkohol. J für Praktische Chemie 5(1):457–464. https://doi.org/10.1002/prac.18720050148
3. Dias TA, Duarte CL, Lima CF, Proença MF, Pereira-Wilson C (2013) Superior anticancer activity of halogenated chalcones and flavonols over the natural flavonol quercetin. Eur J Med Chem 65(0):500–510. https://doi.org/10.1016/j.ejmech.2013.04.064
4. Peng W, Jiabin Y, Jin CAI, Chunlong SUN, Lushen LI, Min JI (2013) An efficient and facile synthesis of flavanones catalyzed by *N*-methylimidazole. J Serb Chem Soc 78(7):917–920. https://doi.org/10.2298/JSC120629157W
5. Slabber CA (2014) The war against pain: the design, synthesis, and testing of potential COX-2 selective inhibitors. University of KwaZulu-Natal, Pietermaritzburg
6. Synthetic biology (2013) Forcing fluorine into molecules. Nature 501(7466):139–139. https://doi.org/10.1038/501139b
7. Hunter L (2010) The C–F bond as a conformational tool in organic and biological chemistry. Beilstein J Org Chem 6:38. https://doi.org/10.3762/bjoc.6.38
8. Filler R, Saha R (2009) Fluorine in medicinal chemistry: a century of progress and a 60-year retrospective of selected highlights. Future Med Chem 1(5):777–791. https://doi.org/10.4155/fmc.09.65
9. Merck E Handbook of instrumental analysis: NMR spectroscopy. E. Merck, Darmstadt
10. Paratone-Parabar. http://hamptonresearch.com/product_detail.aspx?sid=138&pid=404. Accessed 04 Feb 2015
11. MiTeGen. http://www.mitegen.com/. Accessed 04 Feb 2015
12. Incoatec Microfocus Source. http://www.incoatec.de/products/incoatec-microfocus-source-ius/. Accessed 04 Feb 2015
13. Dolomanov OV, Bourhis LJ, Gildea RJ, Howard JAK, Puschmann H (2009) OLEX2: a complete structure solution, refinement and analysis program. J Appl Crystallogr 42(2):339–341. https://doi.org/10.1107/S0021889808042726
14. Sheldrick G (2008) A short history of SHELX. Acta Crystallographica Section A 64(1):112–122. https://doi.org/10.1107/S0108767307043930
15. SADABS (2001) Bruker AXS Inc, Madison, Wisconsin, USA
16. Macrae CF, Edgington PR, McCabe P, Pidcock E, Shields GP, Taylor R, Towler M, van de Streek J (2006) Mercury: visualization and analysis of crystal structures. J Appl Crystallogr 39(3):453–457. https://doi.org/10.1107/S002188980600731X doi
17. Macrae CF, Bruno IJ, Chisholm JA, Edgington PR, McCabe P, Pidcock E, Rodriguez-Monge L, Taylor R, van de Streek J, Wood PA (2008) Mercury CSD 2.0—new features for the visualization and investigation of crystal structures. J Appl Crystallogr 41(2):466–470. https://doi.org/10.1107/S0021889807067908
18. Mohamadi F, Richards NGJ, Guida WC, Liskamp R, Lipton M, Caufield C, Chang G, Hendrickson T, Still WC (1990) Macromodel—an integrated software system for modeling organic and bioorganic molecules using molecular mechanics. J Comput Chem 11(4):440–467. https://doi.org/10.1002/jcc.540110405
19. Schrodinger M (2015) Materials science suite. Schrodinger LLC, New York
20. Schrodinger (2010) The PyMOL molecular graphics system, Version 1.3r1
21. Cason C, Frolich T, Lipka C POV-Ray—the persistence of vision Raytracer. 3.7.0 edn
22. Flack HD, Bernardinelli G (2008) The use of X-ray crystallography to determine absolute configuration. Chirality 20(5):681–690. https://doi.org/10.1002/chir.20473
23. SciFinder (2018) A CAS scientific information solution CAS. https://scifinder.cas.org/. Accessed 26 Jun 2018
24. Ding Y, Yang G-F (2001) Syntheses and fungicidal activity of flavanone derivatives with substitution in B ring. Yingyong Huaxue 18(10):785–789
25. Sakirolla R, Tadiparthi K, Yaeghoobi M, Abd Rahman N (2018) Di-cationic Ionic liquid catalyzed synthesis of 1,5-benzothiazepines. Asian J Chem 30(1):107–115. https://doi.org/10.14233/ajchem.2018.20920
26. Bernstein J, Davis RE, Shimoni L, Chang N-L (1995) Patterns in hydrogen bonding: functionality and graph set analysis in crystals. Angew Chem Int Ed 34(15):1555–1573. https://doi.org/10.1002/anie.199515551
27. Bernstein J, Shimoni L, Davis RE, Chang N-L (1995) Muster aus H-Brücken: ihre Funktionalität und ihre graphentheoretische analyse in kristallen. Angew Chem 107(15):1689–1708. https://doi.org/10.1002/ange.19951071505

28. Marais JPJ, Deavours B, Dixon RA, Ferreira D (2006) The stereochemistry of flavonoids. In: Grotewold E (ed) The science of flavonoids. Springer New York, pp 1–46
29. Bible RH (1965) Interpretation of NMR spectra: an empirical approach. Plenum Press, New York
30. Weigend F, Ahlrichs R (2005) Balanced basis sets of split valence, triple zeta valence and quadruple zeta valence quality for H to Rn: design and assessment of accuracy. Phys Chem Chem Phys 7(18):3297–3305. https://doi.org/10.1039/B508541A
31. David F (1996) The role of databases in support of computational chemistry calculations. J Comput Chem 17(13):1571–1586
32. Schuchardt KL, Didier BT, Elsethagen T, Sun L, Gurumoorthi V, Chase J, Li J, Windus TL (2007) Basis set exchange: a community database for computational sciences. J Chem Inf Model 47(3):1045–1052. https://doi.org/10.1021/ci600510j
33. Adamo C, Barone V (1998) Exchange functionals with improved long-range behavior and adiabatic connection methods without adjustable parameters: the mPW and mPW1PW models. J Chem Phys 108(2):664–675. https://doi.org/10.1063/1.475428
34. Official Gaussian Website. http://www.gaussian.com/. Accessed 26 Apr 2015
35. Frisch MJ, Trucks GW, Schlegel HB, Scuseria GE, Robb MA, Cheeseman JR, Scalmani G, Barone V, Mennucci B, Petersson GA, Nakatsuji H, Caricato M, Li X, Hratchian HP, Izmaylov AF, Bloino J, Zheng G, Sonnenberg JL, Hada M, Ehara M, Toyota K, Fukuda R, Hasegawa J, Ishida M, Nakajima T, Honda Y, Kitao O, Nakai H, Vreven T, Montgomery JA Jr, Peralta JE, Ogliaro F, Bearpark MJ, Heyd J, Brothers EN, Kudin KN, Staroverov VN, Kobayashi R, Normand J, Raghavachari K, Rendell AP, Burant JC, Iyengar SS, Tomasi J, Cossi M, Rega N, Millam NJ, Klene M, Knox JE, Cross JB, Bakken V, Adamo C, Jaramillo J, Gomperts R, Stratmann RE, Yazyev O, Austin AJ, Cammi R, Pomelli C, Ochterski JW, Martin RL, Morokuma K, Zakrzewski VG, Voth GA, Salvador P, Dannenberg JJ, Dapprich S, Daniels AD, Farkas Ö, Foresman JB, Ortiz JV, Cioslowski J, Fox DJ (2009) Gaussian 09 Rev. C.01
36. Mohr PJ, Newell DB, Taylor BN (2016) CODATA recommended values of the fundamental physical constants: 2014. Rev Mod Phys 88:035009–035073. https://doi.org/10.1103/RevModPhys.88.035009
37. Murray-Rust P, Stallings WC, Monti CT, Preston RK, Glusker JP (1983) Intermolecular interactions of the carbon–fluorine bond: the crystallographic environment of fluorinated carboxylic acids and related structures. J Am Chem Soc 105(10):3206–3214. https://doi.org/10.1021/ja00348a041
38. Thalladi VR, Weiss H-C, Bläser D, Boese R, Nangia A, Desiraju GR (1998) C–H···F interactions in the crystal structures of some fluorobenzenes. J Am Chem Soc 120(34):8702–8710. https://doi.org/10.1021/ja981198e
39. Rybalova TV, Bagryanskaya IY (2009) C–F···p. F···H, and F···F intermolecular interactions and F-aggregation: role in crystal engineering of fluoroorganic compounds. J Struct Chem 50(4):741–753
40. Rowland RS, Taylor R (1996) Intermolecular nonbonded contact distances in organic crystal structures: comparison with distances expected from van der Waals Radii. J Phys Chem 100 (18):7384–7391. https://doi.org/10.1021/jp953141&%23x002B;